A GENERIC FINITE ELEMENT IMPLEMENTATION OF ARTERIAL WALL CONSTITUTIVE LAWS

Santiago A. Urquiza[a,c]**, Pablo J. Blanco**[b,c]**, Gonzalo D. Ares**[a] **and Raúl A. Feijóo**[b,c]

[a]*Departamento de Mecánica, Universidad Nacional de Mar del Plata, Av. J.B. Justo 4302, B7608FDQ, Mar del Plata, Argentina, santiago.urquiza@fi.mdp.edu.ar, http://www.fi.mdp.edu.ar/*

[b]*Laboratório Nacional de Computação Científica, Av. Getúlio Vargas 333, Quitandinha, 25651–075, Petrópolis, Brazil, pjblanco@lncc.br, feij@lncc.br, http://www.lncc.br/*

[c]*Instituto Nacional de Ciência e Tecnologia em Medicina Assistida por Computação Científica, Brazil, http://www.lncc.br/prjhemo/*

Keywords: Hyper-elastic, Hemodynamic, Biological Tissues, Models.

Abstract. Hyper-elastic formulations are usually employed to represent the constitutive response of biological tissues. Particularly these formulations are often encountered in models assessing the arterial wall behavior. A great number of distinct hyper-elastic laws can be found in the specialized literature devised to represent, at different extents, the mechanical aspects of the arterial tissues. However, no one can be, a priori, considered more suitable than the others. The choice depends on the specific applications and on the type of mechanical response the corresponding models are intended to account for. Consequently, it is convenient to take at hand the possibility of implementing and rapid prototyping different constitutive laws in an easy and reliable manner. Therefore, in this work we describe how to implement a generic Finite Element framework capable to accommodate practically any hyper-elastic material law. This is carried out using a spatial variational formulation for the momentum equation which is linearized by means of a Newton-Raphson scheme. The iterative algorithm is such that for a given load, the equilibrium is reached in the deformed spatial configuration. The main feature of our approach is based on the evaluation of the second order stress tensor and of the fourth order constitutive tangent tensor using finite differences. That is, given a strain energy potential we compute, by means of a second order finite difference centered scheme, the first (stress) and second (tangent matrix) derivatives. In this way, a generic computational implementation in the context of Finite Elements is achieved, making possible to change the material behavior just changing the procedure that evaluates the elastic function and reusing the entire numerical element structure. The developments are carried out for cuasi-incompressible materials, and some implementation issues are presented and discussed. The method is validated for two common constitutive laws of the arterial tissues including the mechanical response of the arterial wall considered as a fiber-reinforced multilayer material.

1 INTRODUCTION

In recent decades there has been growing scientific interest in the development of constitutive equations representing the mechanical behavior of arterial wall tissues. Such interest is based in the fact that the mechanical response of arteries is related to the onset and development of certain pathologies, such as atherosclerosis. Moreover, the need for complex equations representing the arterial stress-strain relationship arises naturally when modeling efforts are directed to surgical planning of vessel repairs such as bypass grafts and the placement of stents.

Modeling arterial blood flows implies a fluid-structure interaction problem between the arterial walls and the blood inside them. The authors have been working from the last 10 years in Coupled Hetero-dimensional Finite Element problems aimed to model the arterial blood flow in compliant vessels (Urquiza et al., 2006; P. J. Blanco and Urquiza, 2007; Blanco et al., 2009; P. J. Blanco and Feijóo, 2010). Up today, very simple wall models were considered (consistent with the 1D model -independent rings models-). More realistic arterial wall models are needed to be implemented if we are, for example, dealing with models of aneurysms onset, development and rupture.

When implementing a computer code that takes into account appropriate constitutive equations of the arterial tissues, the developer is faced to the fact that there is a broad spectrum of available laws representing the material behavior (A. Delfino and Meister. (1997); Holzapfel (2000); Humphrey and Canham. (2000); M. A. Zulliger (2004)). In this sense, it is difficult to determine a priori, which ones are the best suited for computational models of hemodynamic problems. Observe that, it is mistimed to define in advance which equations should be implemented in the program code, as this would restrict the freedom of choice of the constitutive law which best suits the actual type of the problem to be solved. Furthermore, if the specific material relationships are directly encoded in the Element calculations, the complete Element must be re-coded each time the constitutive law is changed. The key aspect in order to achieve a generic code, is to split the Geometric non-linearities from the Constitutive non-linearities and to encapsulate the Constitutive laws in specific functions embodying the material response.

Thus, in this paper are presented the main conceptual aspects of an Finite Element implementation capable of solving problems of large deformations and displacements, coded in such a way that changes in the constitutive equation does not affect the implementation. This is achieved in a very simple manner through the encapsulation of the constitutive relationships in certain functions used to calculate the tangent matrix components. This brings about a code that separates the constitutive issues from the geometric ones at the same time that encapsulates and simplifies the software coding of material behavior laws. In the hyper-elastic case treated here, the stresses and tangential component of the elastic tensor is obtained by finite differences. So, it is possible to incorporate new material only through programming a scalar function, i.e., the hyper-elastic strain energy potential. Consequently, this impacts on the simplicity of the implementation facilitating and accelerating the way the constitutive laws can be incorporated to the existing software.

2 EQUILIBRIUM AND LINEARIZATION

In this section, the basic large strain mechanical equilibrium equations for an hiper-elastic material (Gurtin, 1981) representing the arterial tissues are presented.

2.1 Spatial and material equilibrium expressions

Considering the arterial tissues as a solid material, the mechanical equilibrium is defined by the following variational problem: find $\mathbf{u}_s \in \mathcal{U}_s$ such that the stress state $\boldsymbol{\sigma}_s$ is such that

$$\int_{\Omega_s} \boldsymbol{\sigma}_s \cdot \hat{\boldsymbol{\varepsilon}}_s \, \mathrm{d}\Omega_s = \int_{\Omega_s} \rho_s \mathbf{f}_s \cdot \hat{\mathbf{v}}_s \, \mathrm{d}\Omega_s + \int_{\Gamma_{Ns}} \mathbf{g}_s \cdot \hat{\mathbf{v}}_s \, \mathrm{d}\Gamma_s \qquad \forall \hat{\mathbf{v}}_s \in \hat{\mathcal{V}}_s, \tag{1}$$

where ρ_s is the density, Γ_{Ns} is the Neumann surface in its spatial configuration whose coordinates are $\mathbf{y}_s = \mathbf{x}_s|_{\Gamma_{Ns}}$. Here, $\mathbf{f}_s$ is a volume loading defined in the current configuration Ω_s, while $\mathbf{g}_s$ is a surface loading acting on the surface Γ_{Ns}. The linear manifold $\mathcal{U}_s$ and its associated linear space $\hat{\mathcal{V}}_s$ are

$$\begin{aligned} \mathcal{U}_s &= \{\mathbf{u}_s \in \mathbf{H}^1(\Omega_s); \ \mathbf{u}_s = \bar{\mathbf{u}}_s \text{ on } \Gamma_{Ds}\}, \\ \hat{\mathcal{V}}_s &= \{\hat{\mathbf{v}}_s \in \mathbf{H}^1(\Omega_s); \ \hat{\mathbf{v}}_s = 0 \text{ on } \Gamma_{Ds}\}. \end{aligned} \tag{2}$$

In the present work we assess the mechanical equilibrium by means of the linearized version of the spatial formulation (1).

2.2 Linearization procedure

For the linearization we make use of the Newton-Raphson method. The linearization of variational formulation (1) is carried out by writing it in the material counterpart, linearizing there and going back to the spatial configuration. For the simplicity in the presentation we disregard the nonlinearities arinsing from the nature of the loadings $\mathbf{f}_s$ and $\mathbf{g}_s$.

Notice that the variational formulation (1) can be written in abstract form as: find $\mathbf{u}_s \in \mathcal{U}_s$ such that

$$\langle \mathcal{R}_{\Omega_s}(\mathbf{u}_s), \hat{\mathbf{v}}_s \rangle_{\Omega_s} = 0 \qquad \forall \hat{\mathbf{v}}_s \in \hat{\mathcal{V}}_s, \tag{3}$$

where in the operator $\mathcal{R}_{\Omega_s}$ the constitutive response and the loading are taken into account. Also this operator depends on the spatial coordinates $\mathbf{x}_s$, and that is why we use the index Ω_s to introduce this dependence. The Newton-Raphson linearization applied to this expression reads as next: find $\delta\mathbf{u}_s \in \mathcal{U}_s$ such that

$$\langle \mathcal{R}_{\Omega_s}(\mathbf{u}_s), \hat{\mathbf{v}}_s \rangle_{\Omega_s} + \frac{\mathrm{d}}{\mathrm{d}\tau} \langle \mathcal{R}_{\Omega_s + \tau\delta\Omega_s}(\mathbf{u}_s + \tau\delta\mathbf{u}_s), \hat{\mathbf{v}}_s \rangle_{\Omega_s + \tau\delta\Omega_s} \bigg|_{\tau=0} = 0$$
$$\forall \hat{\mathbf{v}}_s \in \hat{\mathcal{V}}_s, \quad (4)$$

where $\delta\Omega_s$ denotes the variation of the domain due to the displacement $\delta\mathbf{u}_s$. Therefore, the linear problem consists in finding $\delta\mathbf{u}_s \in \mathcal{U}_s$ such that

$$\langle \mathcal{D}_{\Omega_s}(\mathbf{u}_s)\delta\mathbf{u}_s, \hat{\mathbf{v}}_s \rangle_{\Omega_s} = -\langle \mathcal{R}_{\Omega_s}(\mathbf{u}_s), \hat{\mathbf{v}}_s \rangle_{\Omega_s} \qquad \forall \hat{\mathbf{v}}_s \in \hat{\mathcal{V}}_s, \tag{5}$$

where $\mathcal{D}_{\Omega_s}(\mathbf{u}_s)$ is the tangent operator. In the most general situation this operator accounts for constitutive, geometrical and loads nonlinearities. The tangent operator arises from the second term in the left hand side of (5), so we must provide this expression in order to characterize all the elements present in such equation (5).

After a little of algebra we find that

$$\langle \mathcal{D}_{\Omega_s}(\mathbf{u}_s)\delta\mathbf{u}_s, \hat{\mathbf{v}}_s \rangle_{\Omega_s} = \int_{\Omega_s} \left[\frac{1}{\det \mathbf{F}_s} \mathbf{F}_s \left(\frac{\partial \mathbf{S}_m}{\partial \mathbf{E}_m} \right)_s \mathbf{F}_s^T \boldsymbol{\varepsilon}_s(\delta\mathbf{u}_s) \mathbf{F}_s \mathbf{F}_s^T \cdot \hat{\boldsymbol{\varepsilon}}_s(\hat{\mathbf{v}}_s) \right.$$
$$\left. + (\nabla_{\mathbf{x}_s} \delta\mathbf{u}_s) \boldsymbol{\sigma}_s \cdot (\nabla_{\mathbf{x}_s} \hat{\mathbf{v}}_s) \right] \mathrm{d}\Omega_s. \quad (6)$$

Using the notation

$$\mathbf{D}_s \boldsymbol{\varepsilon}_s(\delta \mathbf{u}_s) = \frac{1}{\det \mathbf{F}_s} \mathbf{F}_s \left(\frac{\partial \mathbf{S}_m}{\partial \mathbf{E}_m} \right)_s \mathbf{F}_s^T \boldsymbol{\varepsilon}_s(\delta \mathbf{u}_s) \mathbf{F}_s \mathbf{F}_s^T, \tag{7}$$

we formulate the linear problem as follows: find $\delta \mathbf{u}_s \in \mathcal{U}_s$ such that

$$\int_{\Omega_s} \left[\mathbf{D}_s \boldsymbol{\varepsilon}_s(\delta \mathbf{u}_s) \cdot \hat{\boldsymbol{\varepsilon}}_s + (\nabla_{\mathbf{x}_s} \delta \mathbf{u}_s) \boldsymbol{\sigma}_s \cdot (\nabla_{\mathbf{x}_s} \hat{\mathbf{v}}_s) \right] \mathrm{d}\Omega_s =$$

$$- \int_{\Omega_s} \boldsymbol{\sigma}_s \cdot \hat{\boldsymbol{\varepsilon}}_s \, \mathrm{d}\Omega_s + \int_{\Omega_s} \rho_s \mathbf{f}_s \cdot \hat{\mathbf{v}}_s \, \mathrm{d}\Omega_s + \int_{\Gamma_{Ns}} \mathbf{g}_s \cdot \hat{\mathbf{v}}_s \, \mathrm{d}\Gamma_s \qquad \forall \hat{\mathbf{v}}_s \in \hat{\mathcal{V}}_s. \tag{8}$$

The first term in the left hand side is derived from the constitutive response, and in components it reads

$$[\mathbf{D}_s]_{ijkl} = \frac{1}{\det \mathbf{F}_s} [\mathbf{F}_s]_{ia} [\mathbf{F}_s]_{jb} [\mathbf{F}_s]_{kc} [\mathbf{F}_s]_{ld} \left(\left(\frac{\partial \mathbf{S}_m}{\partial \mathbf{E}_m} \right)_s \right)_{abcd}. \tag{9}$$

In turn, the second term in the left hand side is the contribution to the tangent matrix of the geometrical nonlinearity resulting from the fact that the configuration is unknown. Evidently, the fourth order tensor $\mathbf{D}_s$ and the Cauchy stress tensor $\boldsymbol{\sigma}_s$ depend upon the current configuration, that is $\mathbf{D}_s = \mathbf{D}_s(\mathbf{u}_s)$ and $\boldsymbol{\sigma}_s = \boldsymbol{\sigma}_s(\mathbf{u}_s)$.

Given the tangent matrix and the stress state, problem (8) constitutes a single step in the iterative algorithm by which the equilibrium is achieved.

2.3 Strain-stress relations and tangent operators

The relation between strain and stress in hyperelastic materials like those treated in the present work is accounted for through the definition of the strain energy function. This potential is a function of the current strain level. Then, let us consider the classical energy strain function ψ depending upon the Green-Lagrange deformation tensor $\psi(\mathbf{E}_m)$. Therefore, the Piola-Kirchhoff stress tensor $\mathbf{S}_m$ is obtained as

$$\mathbf{S}_m = \frac{\partial \psi}{\partial \mathbf{E}_m}, \tag{10}$$

from which it is

$$\boldsymbol{\sigma}_m = \frac{1}{\det \mathbf{F}_m} \mathbf{F}_m \frac{\partial \psi}{\partial \mathbf{E}_m} \mathbf{F}_m^T. \tag{11}$$

In turn, the stiffness tensor (fourth order tensor denoted by $\mathbf{K}_m$) associated with a certain level of strain, say $\mathbf{E}_m$, is obtained by doing

$$\mathbf{K}_m = \frac{\partial \mathbf{S}_m}{\partial \mathbf{E}_m} = \frac{\partial^2 \psi}{\partial \mathbf{E}_m \partial \mathbf{E}_m}, \tag{12}$$

which, according to this notation, it is described in the material configuration.

With this the expressions of the tangent matrix and Cauchy stress in the current configuration and in components are the following

$$[\mathbf{D}_s]_{ijkl} = \frac{1}{\det \mathbf{F}_s} [\mathbf{F}_s]_{ia} [\mathbf{F}_s]_{jb} [\mathbf{F}_s]_{kc} [\mathbf{F}_s]_{ld} \left(\left(\frac{\partial^2 \psi}{\partial \mathbf{E}_m \partial \mathbf{E}_m} \right)_s \right)_{abcd}. \tag{13}$$

$$[\boldsymbol{\sigma}_s]_{ij} = \frac{1}{\det \mathbf{F}_s} [\mathbf{F}_s]_{ik} \left(\left(\frac{\partial \psi}{\partial \mathbf{E}_m} \right)_s \right)_{kl} [\mathbf{F}_s]_{jl}. \tag{14}$$

Observe that, for a given configuration for which we have $\mathbf{F}_m$ at hand (and so $\mathbf{E}_m$) we would have to compute the tangent matrix $\mathbf{K}_m$ and the stress tensor $\mathbf{S}_m$ deriving ψ using (12) and (10), respectively. Then, these quantities must be consistently transformed to the current configuration using equations (13) and (14), respectively.

In view of the wide range of constitutive characterizations for arterial tissues found in the literature, the implementation of the finite strain problem becomes untractable from the point of view of the effort invested in coding expressions like the ones seen above in *ad hoc* situations. It is at this point that the present work presents its major contribution. We propose computing $\mathbf{D}_s$ and $\boldsymbol{\sigma}_s$ by finite differences, as will be seen in Section 3.

3   CALCULATION OF THE TANGENT MATRIX AND THE STRESS STATE

As said above, we need to provide the expressions for $\mathbf{D}_s$ and $\boldsymbol{\sigma}_s$, or $\mathbf{D}_s^D$ and $\boldsymbol{\sigma}_s^D$, respectively. Whitin the context of biomechanics modeling several potential functions are available to represent the constituve behavior of tissues. Indeed, the tissue engineering area has flourished in the last ten years, which has been put in evidence through the proliferation of new constitutive expressions acounting for different sorts of fiber-reinforced material (M. A. Zulliger (2004)). This issue may become a major disadvantage if the computational implementation is not adequately coded. This is because as soon as a different potential function is required for modelling purposes, the element programming code should be completely rewritten if the expressions of its derivatives are embedded and spreaded along the entire code. In this manner, it is convenient to encapsulate the expresions for the energy potential and its derivatives behind software interfaces that isolate it from the main part of the element code where the general geometric aspects are considered. Proceding in this manner, it easely concluded that the programing structure can be further simplified if only the expresion for the elastic energy is required and its first and second derivatives are evaluated by finite differences. In view of this, in this section we introduce a finite difference approach for the calculation of the tangent matrix and the stress tensor. Consequently, the constitutive behavior is easily characterized just by providing the strain energy potential ψ (or ψ^D for incompressible materials), being the tangent and stress tensors computed through several evaluations of this potential. Thus, the entire element code is re-used to evaluate the mechanical equilibrium, and the only procedure to be changed when implementing a new constitutive law is that for the few lines where the expression of the potential ψ is coded. Evidently, this *generic programming* concept makes the constitutive model prototyping a quick and easy step towards assessing and comparing different constitutive models, which in the other hand, are in continuous and increasing development as can be observed in the current biomechanics literature.

As stated above, the finite difference expresion for the constituve tensor and the second Piola-Kirchhoff must be given as derivatives of the potential function.

Let us consider that the constitutive behavior is given by the strain energy potential ψ, which is a function of the Green-Lagrange tensor $\mathbf{E}_m$. Then, the quantities to be evaluated are the following

$$\frac{\partial\psi}{\partial\mathbf{E}_m} \qquad \text{and} \qquad \frac{\partial^2\psi}{\partial\mathbf{E}_m\partial\mathbf{E}_m}. \tag{15}$$

The finite difference approach consists in evaluating the potential ψ at different strains denoted by $\mathbf{E}_m + \Delta\mathbf{E}_m$. It is important to note that being $\mathbf{E}$ a symmetric tensor the corresponding functional form of ψ must be symmetrized or, alternatively, only symmetric perturbations of $\mathbf{E}$ must be considered. Consequently, to evaluate the derivatives, $\mathbf{E}$ will be perturbed preserving

its symmetry. Thus we define the following nine symmetric second order tensorial pertubations:

$$(\mathbf{\Delta}^{KL})_{ij} = \frac{1}{2}\left(\delta_{iK}\delta_{jL} + \delta_{iL}\delta_{jK}\right)\varepsilon$$

where (i,j) are the indices of the tensor $\mathbf{\Delta}^{KL}$, and K, L fixed indicate its perturbed components. Observe that the above expression represent a second order tensor whose non nule components are for the indices (k,l) and (l,k) and is not the expression for a fourth order tensor. Then it is posible to introduce the usefull abreviated notation:

$$\psi^{(\pm KL)} = \psi(\mathbf{E} \pm \mathbf{\Delta}^{KL})$$

$$\psi^{(\pm KL, \pm MN)} = \psi(\mathbf{E} \pm \mathbf{\Delta}^{KL} \pm \mathbf{\Delta}^{MN})$$

$$\psi^{(0)} = \psi(\mathbf{E})$$

And finally it is possible to give the finite difference aproximation for $\mathbf{S}$ as

$$S_{kl} = \frac{\partial\psi}{\partial E_{kl}} \simeq \frac{\psi^{(+KL)} - \psi^{(-KL)}}{2\varepsilon}. \tag{16}$$

In the same manner, the *diagonal* components of $\mathbf{K}$, denoted by $(\mathbf{K})_{klkl} = K_{klkl}, \forall k, l$, are given by

$$K_{klkl} = \frac{\partial^2\psi}{\partial E_{kl}^2} \simeq \frac{\psi^{(+KL)} - 2\psi^{(0)} + \psi^{(-KL)}}{\varepsilon^2}. \tag{17}$$

Analogously, the *cross* derivatives (say $k \neq m$ or $l \neq n$) are calculated as follows

$$K_{klmn} = \frac{\partial^2\psi}{\partial E_{kl}\partial E_{mn}} \simeq$$

$$\frac{\psi^{(+KL,+MN)} - \left[\psi^{(-KL,+MN)} + \psi^{(+KL,-MN)}\right] + \psi^{(-KL,-MN)}}{4\varepsilon^2}. \tag{18}$$

It is quite obvious that the above expresions are equivelent to aproximate the potential ψ as a quadratic function around $\mathbf{E}$, implying a moving least squares cuadratic aproximation with the minimun number of points required to become well defined. Embeding this ideas in a Finite Element code is a straightforward task. As the energy potentials are smooth in the components of $\mathbf{E}$, the precision in the derivative calculation is not an obstacle as far as the evaluation may be made for small enough ε without any numerical impediments. So, a unique code can deal with virtually any hiperelastic material by means of a "black box" procedure being called by the element code with the unique purpose of evaluating $\psi(\mathbf{E})$. In consequence, if another material law is needed, this last procedure may be easely changed as required.

4 TEST CASES

4.1 Test Case 1: Human carotid artery modeled with strain energy function proposed by Delfino

Brief description of proposed constitutive law

This simplified arterial wall constitutive law due to A. Delfino and Meister. (1997) represents an isotropic rubber-like potential for human carotid arteries wich is able to model the typicall

stiffening effects in the high pressure domain. As we know, the strain energy function (SEF) depends on the system´s invariants. In this case, the first invariant $(\overline{I_1} = \overline{C} : I)$ is the only variable of the SEF:

$$\overline{\psi} = \frac{a}{b} \left\{ exp \left[\frac{b}{2} \left(\overline{I_1} - 3 \right) \right] - 1 \right\}$$

Where $a > 0$ is a stress-like material parameter and $b > 0$ is a non-dimensional parameter.

For more details of the mathematical aspects of this formulation, see A. Delfino and Meister. (1997) and Holzapfel (2000).

Model Analysis

Here we have modeled a human carotid artery as a 3D simulation example. Geometrical data and characteristic parameters of the SEF were extracted from the literature cited above.

In table 1 we show the material and geometrical data used in the simulation:

Material Parameters		Geometrical Data	
$a[kPa]$	44.2	Inner Radius [mm]	3.1
b	16.7	External Radius [mm]	4.0

Table 1: Test Case 1. Material parameters and geometrical data

Mesh

A linear tetrahedral mesh was used for the solid, and linear triangles on the surface mesh. It contains 32 elements on the perimeter, 4 elements on the radial direction, and 2 elements on the axial direction. This makes a total of 1536 tetrahedral elements for the solid layer, 128 triangular elements in the interior and exterior surfaces and 256 triangular elements on the top and bottom surfaces.
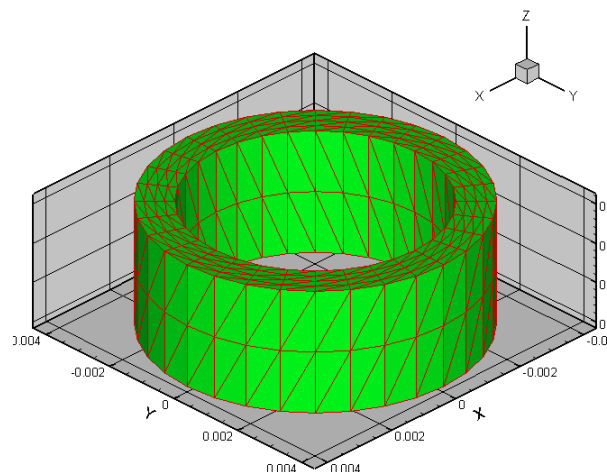

Figure 1: Test Case 1. Mesh

Boundary Conditions

Dirichlet boundary conditions were imposed on nodes of top and bottom surfaces in order to ensure the pre-stretch requisites in each case. To achieve this, we set the value of the axial displacements on the corresponding nodes.

Newmann boundary conditions were imposed in the inner surface, setting a constant value for the pressure.

Results

This test was carried out with 20% pre-stretch and 20 kPa pressure. The figure 2 shows the deformed configuration and the color scale represents the radial displacements.

Finally, figure 3 shows Pressure vs Inner Radius curves obtained in this work compared with published data (Holzapfel, 2000).
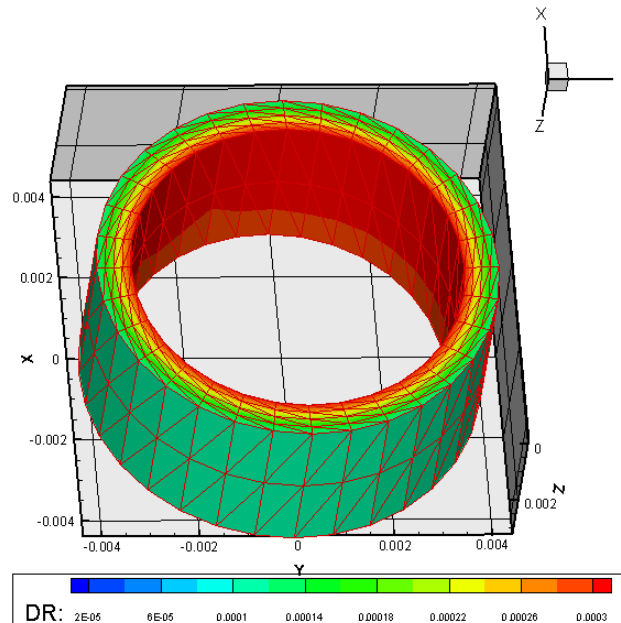

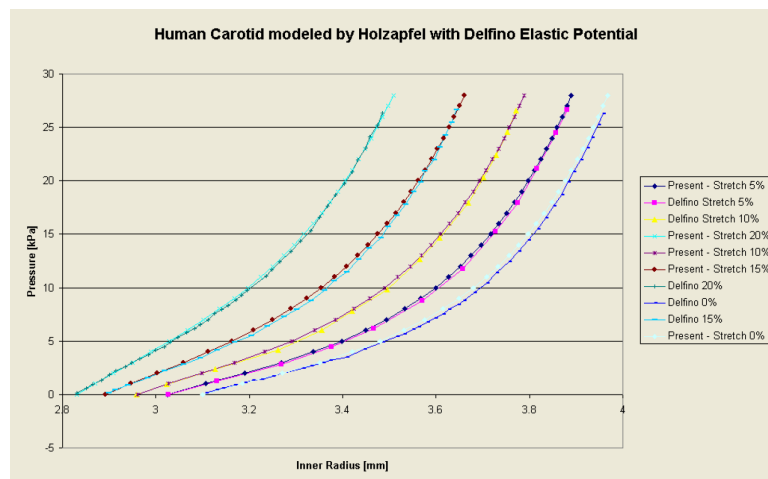
Figure 2: Test Case 1. 3D Example Simulation - 20% pre-stretch and Pressure =20[kPa]

Figure 3: Test Case 1. Pressure vs Inner Radius

4.2   Test Case 2: Rat carotid artery modeled as a multi-layer fiber reinforced material.

Brief description of proposed constitutive law

In this model, Holzapfel (2000) proposed to treat each layer of arterial wall as an isotropic composite reinforced by collagen fibers that act in two main directions. The material parameters are associated with the histological structure of the arterial wall.

Since the artery walls are composed of different layers, each material layer will respond according to an elastic potential. It is assumed that each lamella responds with similar mechanical characteristics. Therefore the same form of the strain energy function is used in both layers, obviouslly, with a different set of parameters in each case. The SEF is separated into an isotropic component, associated with the elastin fibers, and an anisotropic component, which represents the behavior of the collagen fibers. As a result, we can write the SEF as follows:

$$\overline{\psi}(\overline{C}, a_{01}, a_{02}) = \overline{\psi}_{iso}(\overline{C}) + \overline{\psi}_{aniso}(\overline{C}, a_{01}, a_{02})$$

Where $\overline{C}$ is Cauchy tensor and a_{01}, a_{02} the unit vectors that define the collagen fibers directions.

As we know, the potential can only be dependent of the system´s invariants; here we show structure tensors in accordance with the large strain formulation and incorporate two tensors wich contain the information of the collagen fiber directions. Additionally, this information can be put in tensorial form taking the tensorial product of the fiber directions, say, $A_i(i = 1, 2) = a_{oi} \otimes a_{oi}$. For more details, see Holzapfel (2000). Taking into account the following invariants

$$\overline{I}_1(\overline{C}) = tr\overline{C};$$

$$\overline{I}_4(\overline{C}, a_{01}) = \overline{C} : \overline{A}_1; \quad \overline{I}_6(\overline{C}, a_{02}) = \overline{C} : \overline{A}_2$$

it is possible to express the SEF as follows:

$$\overline{\psi}_{iso}(\overline{I}_1) = \frac{c}{2}(\overline{I}_1 - 3)$$

$$\overline{\psi}_{aniso}(\overline{I}_4, \overline{I}_6) = \frac{k_1}{2k_2} \sum_{i=4,6} \left\{ exp[k2(\overline{I}_i - 1)^2] - 1 \right\}$$

Model Analysis

In order to validate the model we simulate a segment of a rat carotid artery and compare the results with the published data found in Holzapfel (2000).

The arterial segment is modeled as a two-layer thick-walled tube with axial pre-stretch. A representative sketch is shown in figure 4. As mentioned before, each layer uses 3 parameters that define the material response. Since arterial walls can be considered as incompresible materials, we use a cuasi-incompresible formulation via sufficient large volumetric modules of elasticity.

Geometrical data and material parameters :

Inner radius: $R_i = 0.71[mm]$

Media thickness: $E_M = 0.26[mm]$

Adventitia thickness: $E_A = 0.13[mm]$

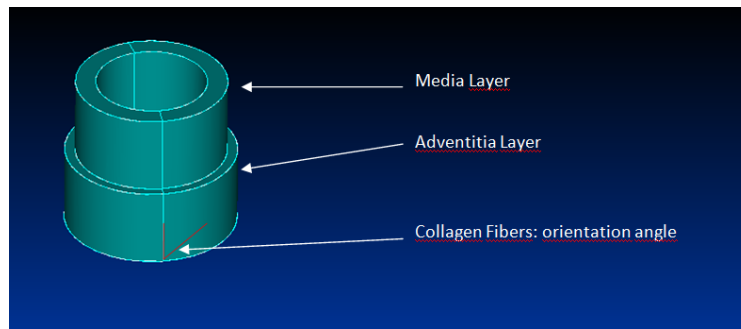The material parameters can be found in table 2 (see (Holzapfel, 2000) for addittional details).

Figure 4: Test Case 2. Layer scheme

Material Parameters		
Parameter	Media	Adventitia
$c[kPa]$	3.0000	0.3000
$k_1[kPa]$	2.3632	0.5620
k_2	0.8323	0.7112
β	61°	28°

Table 2: Test Case 2. SEF Parameters

Mesh

A linear tetrahedral mesh was used for the solid, and linear triangles on the surface mesh. It contains 48 elements on the perimeter, 2 elements on the radial direction for each layer, and 2 elements on the axial direction. This makes a total of 1152 tetrahedral elements for each solid layer, 192 triangular elements in the interior and exterior surfaces and 384 triangular elements on the top and bottom surfaces. The mesh is shown in figure 5.
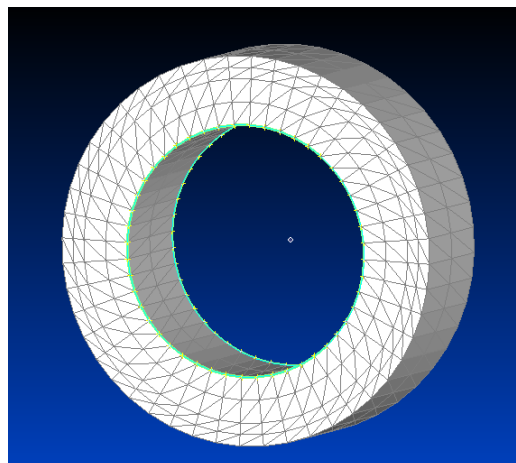

Figure 5: Test Case 2. Mesh

Boundary Conditions

Dirichlet boundary conditions were imposed on nodes of top and bottom surfaces in order to ensure the pre-stretch requisites in each case. To achieve this, we set the value of the axial displacements on the corresponding nodes.

Newmann boundary conditions were imposed in the inner surface, setting a constant value for the pressure.

Results

This test was carried out with 90% pre-stretch and 10 kPa pressure. Figure 6 shows the media layer in the deformed configuration. The color scale represents the radial displacements.

Finally, figure 7 shows Pressure vs Inner Radius curves obtained in this work compared with published data (Holzapfel, 2000).
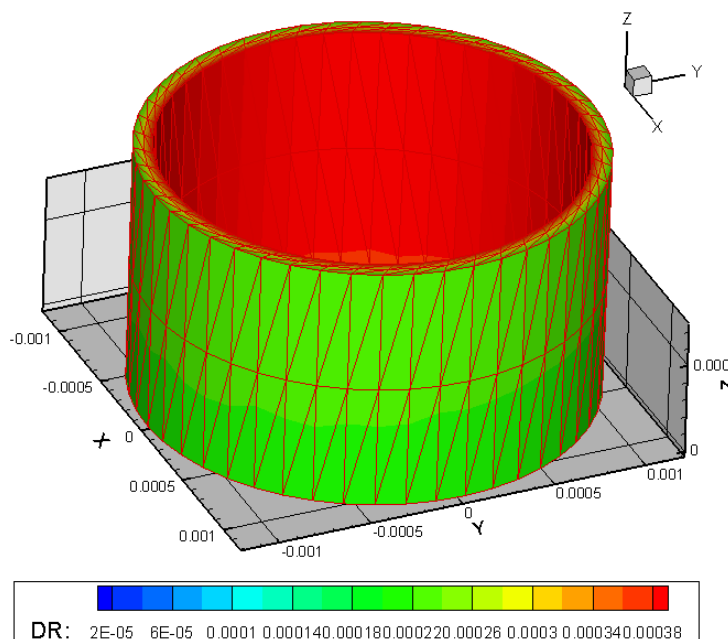

Figure 6: Test Case 2. 3D Example Simulation (media layer) - 90% pre-stretch and Pressure =10[kPa]
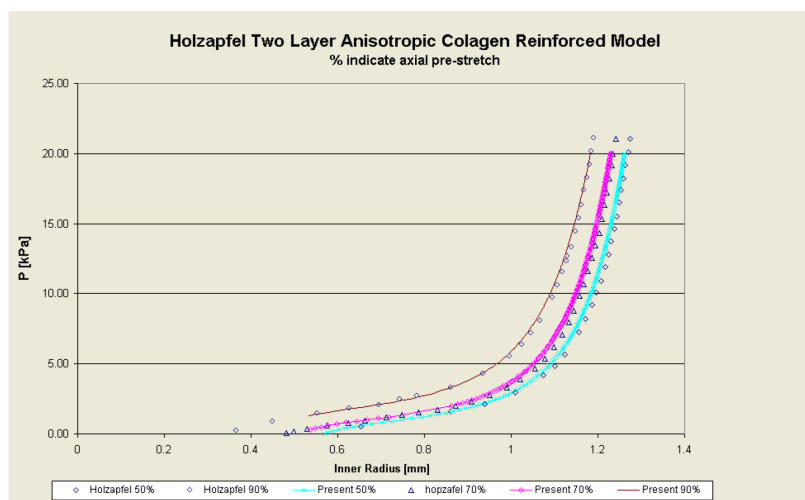

Figure 7: Test Case 2. Pressure vs Inner Radius

5 CONCLUSIONS

In this work we have briefly presented a generic implementation of a Large Strain Formulation capable to deal with virtually any constitutive hiper-elastic law of the arterial wall. The formulation was tested comparing the results with published data for two different cases, both

with good agreement. The approach presented herein provides useful means to represent arterial wall models in an easy a flexible way. Additional work will be required to adapt the present formulation to the truly incompressible case, a subject that is part of the ongoing work of the authors. Our future work in this area will include coupling this formulation with a Navier-Stokes model in compliant domains in order to realistically address problems like the onset and development of aneurisms.

REFERENCES

A. Delfino N. Stergiopulos J.M. and Meister. J.J. Residual strain effects on the stress field in a thick wall finite element model of the human carotid bifurcation. *Journal of Biomechanics*, 30:777–786., 1997.

Blanco P., Pivello M., Urquiza S., and Feijóo R. On the potentialities of 3d-1d coupled models in hemodynamics simulations. *Journal of Biomechanics*, 42(7):919–930, 2009.

Gurtin M.E. *An introduction to continuum mechanics*. Academic Press, 1981.

Holzapfel G.A. G.T. A new constitutive framework for arterial wall mechanics and a comparative study of material models. *Journal of Elasticity*, 61:1–48, 2000.

Humphrey J. and Canham. P. Structure, mechanical properties, and mechanics of intracranial saccular aneurysms. *Journal of Elasticity*, 61:49–81, 2000.

M. A. Zulliger P. Fridez K.H.N.S. A strain energy function for arteries accounting for wall composition and structure. *Journal of Biomechanics*, 37:989–1000, 2004.

P. J. Blanco R.A.F. and Urquiza S.A. A unified variational approach for coupling 3d-1d models and its blood flow applications. *Computer Methods in Applied Mechanics and Engineering*, 1996(41-44):4391–4410, 2007. doi:10.1016/j.cma.2007.05.008.

P. J. Blanco S. A. Urquiza S.A. and Feijóo R. Assessing the influence of heart rate in local hemodynamics through coupled 3d-1d-0d models. *Int. J. Numer. Meth. Biomed. Engng.*, 26:890–903., 2010. doi:10.1002/cnm.1389. Wiley InterScience (www.interscience.wiley.com). Print ISSN: 2040-7939. Online ISSN: 2040-7947.

Urquiza S., Blanco P., Vénere M., and Feijóo R. Multidimensional modeling for the carotid blood flow. *Computer Methods in Applied Mechanics and Engineering*, 195:4002–4017, 2006.